



Hit-to-lead optimization and kinase selectivity of imidazo[1,2-*a*]quinoxalin-4-amine derived JNK1 inhibitors



Bei Li[†], Oana M. Cociorva[†], Tyzoon Nomanbhoy, Helge Weissig, Qiang Li, Kai Nakamura, Marek Liyanage, Melissa C. Zhang, Ann Y. Shih, Arwin Aban, Yi Hu, Julia Cajica, Lan Pham, John W. Kozarich, Kevin R. Shreder^{*}

ActivX Biosciences, Inc., 11025 N. Torrey Pines Road, La Jolla, CA 92037, USA

ARTICLE INFO

Article history:

Received 14 May 2013

Revised 19 June 2013

Accepted 27 June 2013

Available online 8 July 2013

Keywords:

JNK1 inhibitor

Imidazo[1,2-*a*]quinoxalin-4-amine

Kinase profiling

AX13587

AX14373

ABSTRACT

As the result of a rhJNK1 HTS, the imidazo[1,2-*a*]quinoxaline **1** was identified as a 1.6 μ M rhJNK1 inhibitor. Optimization of this compound lead to **AX13587** (rhJNK1 IC₅₀ = 160 nM) which was co-crystallized with JNK1 to identify key molecular interactions. Kinase profiling against 125+ kinases revealed **AX13587** was an inhibitor of JNK, MAST3, and MAST4 whereas its methylene homolog **AX14373** (native JNK1 IC₅₀ = 47 nM) was a highly specific JNK inhibitor.

© 2013 Elsevier Ltd. All rights reserved.

The c-Jun N-terminal kinases (JNKs) are serine/threonine kinases and members of the extensive MAP Kinase family. In mammals there are three JNK genes: JNK1 (four isoforms), JNK2 (four isoforms) and JNK3 (two isoforms).¹ The JNK1 and JNK2 genes are widely expressed, whereas JNK3 expression is restricted to the brain, heart and testis.² JNK activation by extracellular stimuli, such as stress or cytokines, leads to the phosphorylation of several transcription factors and cellular substrates implicated in cell proliferation, cell survival, cell death, DNA repair and metabolism.³ Because these pathways are related to the pathogenesis of several diseases JNKs represent valuable targets in the development of new therapies.⁴ Celgene has disclosed the SAR data, co-crystal structures with JNK3, and in vivo data for the JNK inhibitors CC-359⁵ and CC-930,⁶ the latter of which entered phase II clinical trials for the treatment of idiopathic pulmonary fibrosis.

As the result of a high throughput screen of an internal compound library against recombinant human JNK1 (rhJNK1), three compounds with rhJNK1 IC₅₀ values <10 μ M (**1–3**, Table 1) were found.⁷ These compounds were profiled against a panel of over 125 kinases using the desthiobiotin-tagged ATP probe **AX9989**⁸ as previously described.⁹ After probe-labeling of PC3 lysate in the presence of inhibitors (30 μ M) followed by trypsinization, kinase active site peptides were identified and quantified using LC/MS.

Percent inhibition was calculated as the normalized decrease in the fragment intensities of probe-labeled peptides in samples incubated with inhibitor compared to those without. In cases where the tryptic active site peptide is redundant (e.g., the JNKs) % inhibition cannot be assigned to an individual kinase and multiple kinases appear in a single row (Table 2). Considering the high screening concentration of 30 μ M, this analysis indicated **1–3** were selective inhibitors of the JNK family with few off-targets.

The optimization of the most potent and JNK selective of these hits (**1**) was conducted via the derivatization of 4-chloroimidazo[1,2-*a*]quinoxaline¹⁰. This intermediate was treated with various cyclohexylamine derivatives (TEA (2 equiv), DMSO, 100 °C, 16 h) leading to compounds **4–7** (Table 1). This effort led to the *trans*-hydroxy derivative **7** and an accompanying 1.8- to 9.2-fold increase in the rhJNK1 inhibitory activity relative to compounds **1–6**. While progress was made with respect to potency, kinase profiling indicated that little ground was made in tuning out off-target kinases for compound **7** (Table 2). Nevertheless we moved forward with **7** knowing that at some point we would have to improve JNK selectivity.

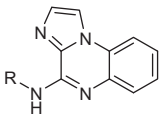
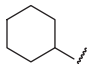
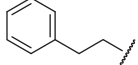
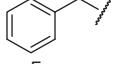
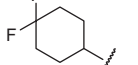
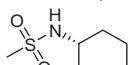
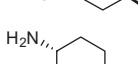
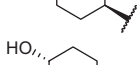
To explore the role of the fused imidazole ring of **7**, two compounds (**8** and **9** in Fig. 1) were synthesized from 4-chloropyrrol-ol[1,2-*a*]quinoxaline¹¹ and 4-chloro-1,2-dihydroimidazo[1,2-*a*]quinoxaline¹² in an analogous fashion to **7** (rhJNK1 IC₅₀ = 0.91 μ M). By comparison to **7**, compounds **8** and **9** had significantly attenuated rhJNK1 inhibitory activities, with rhJNK1 IC₅₀ values of >100 μ M and 73 μ M respectively. This loss in potency indicated

^{*} Corresponding author. Tel.: +1 858 526 2517; fax: +1 858 587 4878.

E-mail address: kevins@activx.com (K.R. Shreder).

[†] These authors contributed equally to this work.

Table 1
rhJNK1 IC₅₀ values of the HTS hits **1–3** and derivatives of **1**

		
Compound	R	rhJNK1 IC ₅₀ (μM)
1 ^a		1.6
2 ^a		6.7
3 ^a		8.4
4		8.0
5		2.4
6		1.7
7 ^a		0.91

^a Profiled against a panel of human kinases (see Table 2).

that the non-bridgehead nitrogen and aromaticity of the fused imidazole ring present in **7** were critical JNK1 binding elements. Accordingly we chose not to make changes to the core imidazo[1,2-*a*]quinoxaline scaffold.

To further increase potency and selectivity, 7- and 8-substituted carboxy and carboxamide derivatives of **7** were explored. The syntheses of 8-substituted derivatives are shown in Scheme 1. When methyl 3-fluoro-4-nitro-benzoate (**10**) and ethyl imidazole-2-carboxylate were heated in the presence of cesium carbonate compound **11** was produced via a S_NAr reaction. When the nitro group of **11** was reduced to the corresponding amine with iron powder in ethanol/water/acetic acid and then subjected to heating, cyclization to form the tricyclic intermediate **12** occurred. Chlorination of **12** to give the 4-Cl intermediate **13** was accomplished using phosphoryl chloride and catalytic *N,N*-dimethylaniline. Com-

Table 2
Kinase selectivity profiling (KiNativ™) of **1–3** and **7** in PC3 lysate showing % inhibition of ATP probe labeling (**AX9989**) of the indicated kinase (leftmost column) at a screening concentration of 30 μM

	1	2	3	7
JNK1,JNK2,JNK3	80.4	41.6	46.2	97.5
MAST3	<35	<35	<35	<35
CDK9	50.7	<35	<35	90.7
PI4KB	55.9	59.9	66.5	90.8
CDK10	37.2	35.7	<35	79.8
PITSLRE	<35	<35	<35	82.4
PIP4K2C	<35	59.4	40.3	51.9
PIP4K2C	<35	52.6	<35	50.9
PEK	<35	<35	<35	65.0
GCN2	<35	<35	<35	41.0
GCN2	<35	<35	<35	36.9
PCTAIRE1	<35	<35	<35	38.9
TAO2	<35	<35	<35	37.0
CK2α2	<35	<35	<35	49.6
LKB1	<35	<35	<35	45.6

Data is shown in the form of a heat map and structures of compounds can be found in Table 1. Over 100 additional kinases were screened but did not show significant inhibition (i.e., <35%). More than one probe labeling site exists for PIP4K2C and

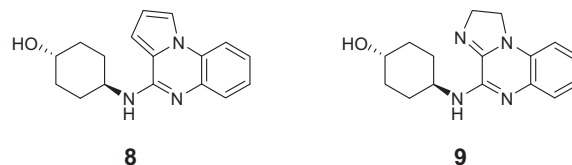
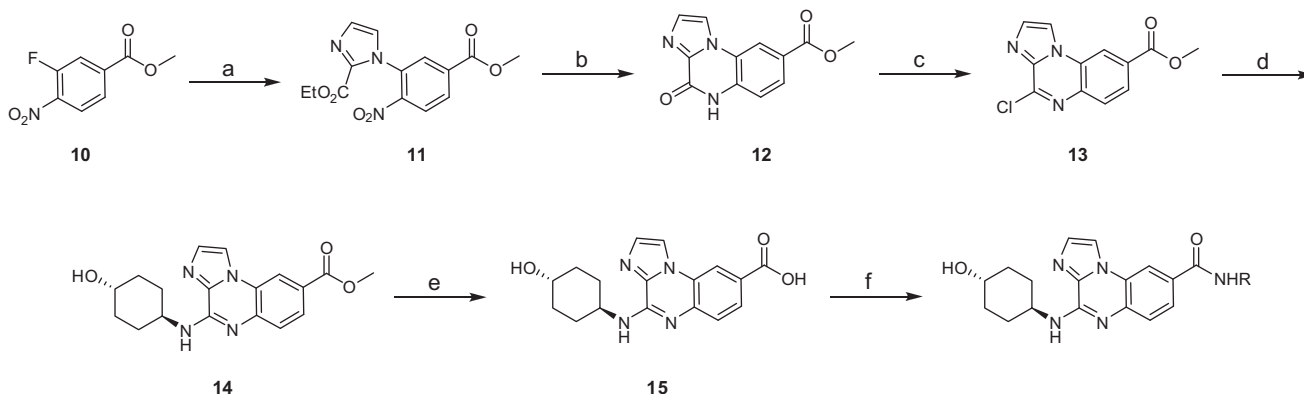


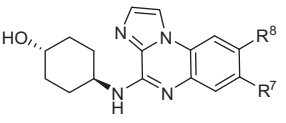
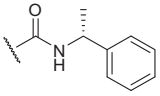
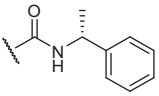
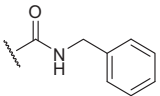
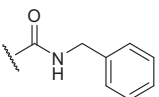
Figure 1. Structure of pyrrolo[1,2-*a*]quinoxaline (**8**) and 1,2-dihydroimidazo[1,2-*a*]quinoxaline (**9**) analogs of **7**.

pound **13** was converted to **14** by treatment with *trans*-4-aminocyclohexanol in DMSO at 120 °C. Hydrolysis of **14** was carried out using aqueous potassium hydroxide in THF to give **15**. Reaction of **15** with primary amines using the carbodiimide EDC at room temperature yielded 8-position amides. 7-substituted carboxy and carboxamide derivatives were synthesized in a similar manner starting from methyl 4-fluoro-3-nitro-benzoate. The rhJNK1 inhib-



Scheme 1. Generalized synthesis of JNK1 inhibitors: (a) ethyl 1H-imidazole-2-carboxylate, Cs₂CO₃, DMF, 55 °C, 70%; (b) iron powder, EtOH:AcOH:H₂O (2:2:1), sonication, 4 h, 62%; (c) POCl₃, *N,N*-dimethylaniline, reflux, 80%; (d) *trans*-4-aminocyclohexanol, TEA, DMSO, 120 °C, 5 h, 95%; (e) KOH/H₂O, THF, 80 °C, 4 h, then HCl, 85%; (f) NH₂R, HOBT, EDC, DMF, rt, 4 h. 7-Substituted derivatives were synthesized in a similar manner from methyl 4-fluoro-3-nitro-benzoate.

Table 3
rhJNK1 IC₅₀ values of 7- and 8-carboxy and carboxamide derivatives of compound 7

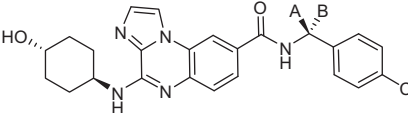
			
Compound	R ⁷	R ⁸	rhJNK1 IC ₅₀ (μM)
15 ^a	H	-COOH	0.31
16	-COOH	H	1.5
17 ^a	H	-CONH ₂	0.57
18	-CONH ₂	H	4.17
19 ^a	H		0.58
20		H	1.5
21	H		0.68
22		H	0.49

^a Profiled against a panel of human kinases (see Table 5).

itory activity of various paired 7- and 8- substituted derivatives of compound 7 were then compared (Table 3). In 3 out of 4 pairs, 8-substitution yielded better rhJNK1 inhibitory activity than the 7-substituted analog (compare **15** vs. **16**, **17** vs. **18**, **19** vs. **20**). For the remaining pair, both compounds **21** and **22** had similar rhJNK1 IC₅₀ values. Finally, all 8-substituted derivatives in Table 3 were more potent than compound 7.

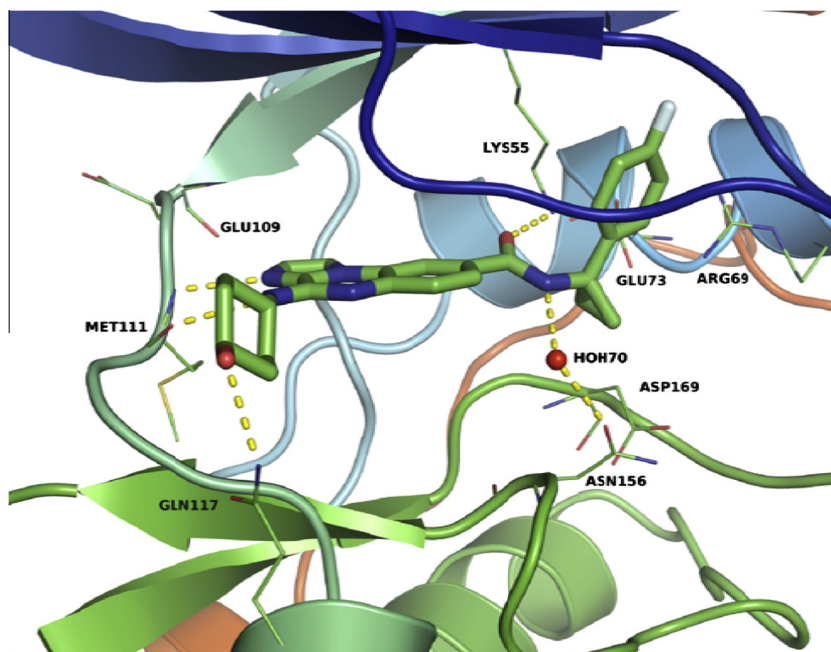
The above data prompted us to further investigate 8-benzylamide derivatives of compound 7 (Table 4). When chiral α-substituted benzylamides were examined (**19**, **23–27**), it was found that amides based on (*R*)-α-methylbenzylamine (**19**) and deriva-

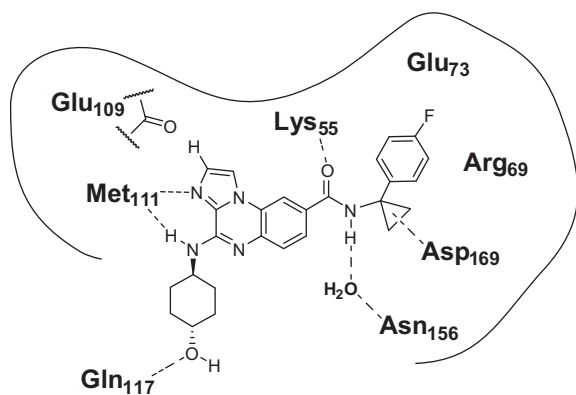
Table 4
rhJNK1 IC₅₀ values of 8-carboxamide derivatives of compound 7

				
	A	B	C	rhJNK1 IC ₅₀ (μM)
23 ^a	Me	H	H	1.98
19 ^a	H	Me	H	0.58
24	Et	H	H	1.7
25 ^a	H	Et	H	0.14
26	CH ₂ OH	H	H	4.9
27 ^a	H	CH ₂ OH	H	0.16
28 ^a	H	CH ₂ CH ₂ CH ₃	H	0.2
29	H	iPr	H	0.35
30	H	Ph	H	0.36
31	H	CH ₂ CH ₂ OH	H	0.62
32	H	CH ₂ OCH ₃	H	0.69
33 ^a	Me	Me	H	0.27
34	Et	Et	H	0.16
35 ^a		CH ₂ CH ₂	H	0.092
36 ^a		CH ₂ CH ₂ CH ₂	H	0.077
37		CH ₂ CH ₂ CH ₂ CH ₂	H	0.18
38		CH ₂ CH ₂ CH ₂ CH ₂ CH ₂	H	1.22
39		CH ₂ CH ₂ CH ₂ CH ₂ CH ₂ CH ₂	H	0.43
40		CH ₂ CH ₂	Me	0.25
41		CH ₂ CH ₂	Cl	0.19
AX13587		CH ₂ CH ₂	F	0.16

^a Profiled against a panel of human kinases (see Table 5).

tives thereof (**25** and **27**) were more potent than their enantiomers (**23**, **24**, and **26**, respectively), by as much as 31-fold (compare **26** versus **27**). Other derivatives of compound **19** (**28–32**) were investigated, but none found as potent as **25** (B = Et, rhJNK1 IC₅₀ = 140 nM). Two achiral α,α-gem-disubstituted benzylamides (**33** and **34**) were examined and only one such compound (**34**, A = B = Et, rhJNK1 IC₅₀ = 160 nM) was of similar potency as **25**. Using the rhJNK1 assay, two spirocyclic compounds **35** (spirocyclopropyl, rhJNK1 IC₅₀ = 92 nM) and **36** (spirocyclobutyl, rhJNK1 IC₅₀ = 77 nM) were found to be the two most potent rhJNK1 inhibitors in this study. Neither increasing the spiroalkyl ring size (**37–39**) nor deriv-

**Figure 2.** Crystal structure of AX13587 in the JNK1 active site (PDB ID: 4L7F).



Scheme 2. Schematic drawing showing the key molecular interactions of the **AX13587**-JNK1 co-crystal structure.

atization of **35** in the *para*-position (C = Me, Cl, F) resulted in an increase in the rhJNK1 inhibitory activity.

To understand better the details of how this class of inhibitor binds, a co-crystal structure of **AX13587** in the JNK1 ATP-binding site was obtained (Fig. 2 and Scheme 2). Selected residues are

highlighted in the JNK1 ATP binding site to illustrate several favorable interactions with the imidazo[1,2-*a*]quinoxaline scaffold, the *trans*-4-hydroxy-hexylamine group, and the 4-fluorophenyl-cyclopropyl-amide moiety: dual hydrogen bond interactions with the hinge region (Met111), hydrogen bonding with the solvent exposed Gln117, a bridged hydrogen bond between a water molecule and Asn156, and a hydrogen bond with the catalytic Lys55. Lipophilic interactions are present between the phenyl ring of the scaffold and the ribose-binding pocket as well as in an induced-fit binding pocket formed by Arg69 and Glu73 and occupied by the fluorophenyl group. This induced-fit pocket is not found in any other JNK co-crystal structures and is absent in the apo structures of JNK isoforms (e.g., PDB ID 1UKH, not shown). The positioning of the inhibitor within this pocket also enables additional hydrophobic interactions between the β -carbon of Asp169 and the cyclopropyl ring of the 8-amide substituent. In total, these interactions explain aspects of the structure–activity relationship of our compound series: the importance of the *trans*-hydroxy group, the improvement of potency when a C8 benzylamide was introduced, and the limited steric tolerance for spirocyclic groups significantly larger than the cyclopropyl group.

Table 5
Kinase selectivity profiling (KiNativ™) of selected JNK1 inhibitors in PC3 lysate showing % inhibition of ATP probe labeling (**AX9989**) of the indicated kinase (leftmost column) at a screening concentration of 10 μ M

	15	17	23	19	25	27	28	33	35	36	AX13587	AX14373
JNK1,JNK2,JNK3	99.1	97.5	86.5	98.2	98.6	98.5	95.3	98.3	99.2	99.2	98.7	99.5
MAST3	<35	<35	76.3	97.0	96.2	97.9	90.2	99.3	98.9	99.2	97.6	<35
CDK10	91.3	90.4	<35	56.2	<35	46.6	<35	<35	<35	59.1	<35	<35
CDK9	97.9	98.6	<35	42.0	<35	<35	<35	<35	<35	49.8	<35	<35
CK1 δ ,CK1 ϵ	81.2	91.3	<35	42.6	<35	<35	<35	<35	<35	<35	44.3	<35
GSK3 β	98.6	96.0	<35	<35	<35	<35	<35	<35	<35	<35	<35	<35
PI4KB	99.2	94.2	<35	40.4	<35	51.0	<35	<35	<35	<35	<35	<35
PIP4K2C	90.1	79.1	<35	55.3	<35	44.5	<35	<35	38.9	<35	<35	<35
PIP4K2C	94.6	78.1	<35	51.0	<35	48.9	<35	<35	<35	<35	39.5	<35
PITSLRE	99.3	95.6	<35	<35	<35	<35	<35	<35	<35	<35	<35	<35
PFTAIRE1	80.1	<35	<35	<35	<35	<35	<35	<35	<35	<35	<35	<35
PRPK	86.6	<35	<35	<35	<35	<35	<35	<35	<35	<35	<35	<35
CDK2	59.1	<35	<35	<35	<35	<35	<35	<35	<35	<35	<35	<35
CK1 α	57.1	69.0	<35	<35	<35	<35	<35	<35	<35	<35	<35	<35
GCN2	54.8	<35	<35	61.7	45.2	59.4	<35	<35	<35	<35	<35	<35
GCN2	41.7	<35	<35	54.0	38.5	56.4	<35	<35	<35	<35	<35	<35
p38 δ ,p38 γ	57.7	44.4	<35	<35	<35	<35	<35	<35	<35	<35	<35	<35
PCTAIRE1	71.1	<35	<35	<35	<35	<35	<35	<35	<35	<35	<35	<35
PEK	37.5	<35	<35	38.4	<35	<35	<35	<35	<35	<35	<35	<35
PI4KA,PI4KAP2	73.1	<35	<35	<35	<35	<35	<35	<35	<35	<35	<35	<35
PKD2	<35	51.7	<35	<35	<35	<35	<35	<35	<35	<35	<35	<35
TAO2	67.0	<35	<35	<35	<35	<35	<35	<35	<35	<35	<35	<35
AMPK α 1,AMPK α 2	<35	<35	<35	45.3	<35	40.1	<35	<35	35.9	<35	<35	<35
AMPK α 1,AMPK α 2	<35	<35	<35	43.2	<35	44.7	<35	36.6	<35	<35	35.8	<35
CaMK2 α ,CaMK2 β ,CaMK2 δ ,CaMK2 γ	<35	<35	<35	<35	46.9	<35	<35	<35	<35	<35	<35	<35
CaMK2 γ	<35	<35	<35	<35	48.7	<35	<35	<35	<35	<35	<35	<35
CHK2	<35	<35	<35	36.9	<35	45.6	<35	<35	<35	<35	<35	<35
CK2 α 2	40.6	<35	<35	<35	<35	<35	<35	<35	<35	<35	<35	<35
LKB1	<35	<35	<35	<35	<35	<35	<35	<35	<35	<35	<35	<35
MPSK1	48.9	39.1	<35	<35	<35	<35	<35	<35	<35	<35	<35	<35
ZC1/HGK,ZC2/TNIK,ZC3/MINK	<35	37.0	<35	<35	<35	<35	<35	<35	<35	<35	<35	<35
IKK ϵ ,TBK1	<35	<35	<35	38.7	<35	<35	<35	<35	<35	<35	<35	<35
PIK3CB	37.1	<35	<35	<35	<35	<35	<35	<35	<35	<35	<35	<35

Data is shown in the form of a heat map and compound structures can be found in Tables 3 and 4. Other kinases that gave <35% inhibition but are not shown in this table can be found in Ref. ¹³. More than one probe labeling site exists for PIP4K2C, GCN2, and AMPK α 1/AMPK α 2, so these kinases appear twice on this table.

Kinase profiling of selected JNK1 inhibitors of different structural subtypes (from Tables 3 and 4, indicated by an asterisk) was conducted at a screening concentration of 10 μ M (Table 5).¹³ Compounds with rhJNK1 IC₅₀ values <600 nM highly inhibited ATP probe labeling of the JNKs (i.e., >97%). In addition, when compared **19** and **23** exhibited the same trend of enantioselective binding observed in the rhJNK1 assay. Interestingly, we found derivatives lacking an 8-benzylamide group (8-COOH: **15** and 8-CONH₂: **17**) to be highly promiscuous, inhibiting >7 kinases by >90% as well as many other kinases in the μ M range (note: at a 10 μ M screening concentration, >90% inhibition is equivalent to an IC₅₀ value <1 μ M). Unexpectedly, chiral and achiral 8-benzylamides (**23**, **19**, **25**, **27**, **28**, **33**, **35**, and **36**) carried MAST3¹⁴ as a common off target. The spirobutyl derivative **36**, identified as the most potent rhJNK1 inhibitor, was also found to be a very potent MAST3 inhibitor. Using a more expansive interrogation of the kinome in HuH-7 lysate, selected 8-benzylamide derivatives were examined and found to be inhibitors of MAST 1/2 and MAST4 (see Table 6). Considering the lack of off-targets other than MAST kinases, these inhibitors are best described as dual JNK/MAST kinase inhibitors. The ability to find inhibitors fortuitously for unexplored kinases (e.g., MAST3) has been cited as one of the many benefits of kinase profiling.¹⁵

Because MAST3 was a persistent off-target for the 8-benzylamide series, we synthesized and explored 8-phenethylamides, including **AX14373**, a methylene homolog of **AX13587** (Fig. 3). Kinase profiling found this simple modification dialed out all MAST kinase inhibitory activity (Table 5 and data not shown). Furthermore **AX14373** was found to be a highly JNK-selective inhibitor; no significant off-targets were seen when profiled against over 200 kinases.

Because our mass spectrometry-based kinase profiling platform cannot deconvolute % inhibition values for individual JNK isoforms, an alternate assay was developed. To determine native JNK1 and JNK2 IC₅₀ values the immunoprecipitation of JNK1 and JNK2 which had been desthiobiotin-tagged with the ATP probe **AX9509**¹⁶ was used. Labeling was conducted in the presence and absence of inhibitors followed by immunoprecipitation with avidin. Probe-labeled proteins were eluted, resolved by 1D-SDS PAGE, and transferred to nitrocellulose. Western blot quantification with JNK1 or JNK2 specific antibodies could then be used to calculate % inhibition of desthiobiotin labeling and subsequently JNK1 or JNK2 IC₅₀ values. This analysis was conducted for selected compounds in this study (see Table 7). Interestingly, in all cases, the native JNK1 IC₅₀ value was lower than that measured with the recombinant form. A result that suggests differences in potency may arise when assays do not take place in the full complement of lysate.

In summary, lead optimization of the hit **1** resulted in both the development of novel JNK/MAST kinase inhibitors and **AX14373**, a

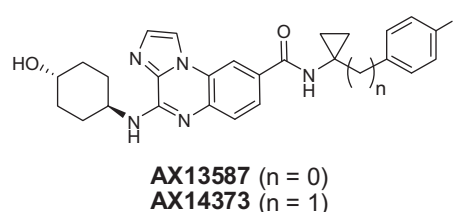


Figure 3. Structures of **AX13587** and **AX14373**.

Table 7

Native JNK1 and JNK2 IC₅₀ values for selected compounds in this study

Compound	Native JNK1 IC ₅₀ (nM)	Native JNK2 IC ₅₀ (nM)
16	82	n.d.
25	33	100
27	67	135
34	59	>190
41	140	>190
AX13587	41	n.d.
AX14373	47	120

Jurkat lysate was used as a source of native JNK1 and JNK2. n.d. = not determined.

highly selective JNK inhibitor. Kinase profiling was used in all phases of this effort from the analysis of hits, understanding the SAR of unintended and unwanted off targets, and finally the confirmation of selectivity for the intended target. Future work describing the optimization and characterization of the 8-phenethylamide series will be published in due course.

References and notes

- Gupta, S.; Barrett, T.; Whitmarsh, A. J.; Julie Cavanagh, J.; Sluss, H. K.; Dérjard, B.; Davis, R. J. *EMBO J.* **1996**, *15*, 2760.
- Martin, J. H.; Mohit, A. A.; Miller, C. A. *Brain Res. Mol. Brain Res.* **1996**, *35*, 47.
- (a) Leppa, S.; Bohmann, D. *Oncogene* **1999**, *18*, 6158; (b) Weston, C. R.; Davis, R. J. *Curr. Opin. Genet. Dev.* **2002**, *12*, 14.
- (a) Manning, A. M.; Davis, R. J. *Nat. Rev. Drug Disc.* **2003**, *2*, 554; (b) Siddiqui, M. A.; Reddy, P. A. *J. Med. Chem.* **2010**, *53*, 3005.
- Plantevin Krenitsky, V.; Delgado, M.; Nadolny, L.; Sahasrabudhe, K.; Ayala, L.; Clareen, S. S.; Hilgraf, R.; Albers, R.; Kois, A.; Hughes, K.; Wright, J.; Nowakowski, J.; Sudbeck, E.; Ghosh, S.; Bahmanyar, S.; Chamberlain, P.; Muir, J.; Cathers, B. E.; Giegel, D.; Xu, L.; Celeridad, M.; Moghaddam, M.; Khatsenko, O.; Omholt, P.; Katz, J.; Pai, S.; Fan, R.; Tang, Y.; Shirley, M. A.; Benish, B.; Blease, K.; Raymon, H.; Bhagwat, S.; Henderson, I.; Cole, A. G.; Bennett, B.; Satoh, Y. *Bioorg. Med. Chem. Lett.* **2012**, *22*, 1427.
- Plantevin Krenitsky, V.; Nadolny, L.; Delgado, M.; Ayala, L.; Clareen, S. S.; Hilgraf, R.; Albers, R.; Hegde, S.; D'Sidocky, N.; Sapienza, J.; Wright, J.; McCarrick, M.; Bahmanyar, S.; Chamberlain, P.; Delker, S. L.; Muir, J.; Giegel, D.; Xu, L.; Celeridad, M.; Lachowitz, J.; Bennett, B.; Moghaddam, M.; Khatsenko, O.; Katz, J.; Fan, R.; Bai, A.; Tang, Y.; Shirley, M. A.; Benish, B.; Bodine, T.; Blease, K.; Raymon, H.; Cathers, B. E.; Satoh, Y. *Bioorg. Med. Chem. Lett.* **2012**, *22*, 1433.
- rhJNK1 IC₅₀ assay: Recombinant histidine-tagged, full-length human, JNK1 (Invitrogen) expressed in insect cells and activated by in vitro phosphorylation by GST-tagged MAP2K7 was used in the assay. Briefly, in a volume of 30 μ L, 70–90 ng of JNK1 enzyme was incubated in the presence or absence of compound at varying concentrations for 1 h at 30 °C in 50 mM Tris, pH 7.5, 10 mM magnesium acetate, 1 mM EGTA, 0.1 μ G/ μ L human recombinant ATF2 (aa19–96, Millipore), 5 μ M ATP, and 1 mM dithiothreitol. Following the completion of the kinase reaction an equal volume of KinaseGlo or KinaseGlo Plus luciferase reagent (Promega) was added and the luminescence was read using a luminescence plate reader within 5–10 min. Compound activity was expressed as % inhibition relative to maximal inhibition observed at the maximal dose. The luminescence readouts from 3 replicates per concentration were averaged to produce a single curve. IC₅₀ values were calculated from this curve using curve fitting software (GraphPad Prism).
- Structure of the desthiobiotin-ATP probe **AX9989**

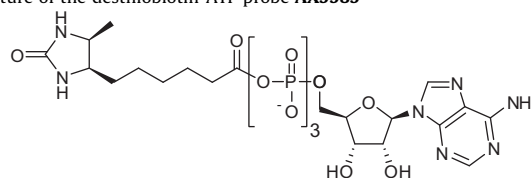


Table 6

MAST family off target activity for selected JNK inhibitors at a screening concentration of 10 μ M in HuH-7 lysate

compound	MAST 1/2 % inhibition	MAST3 % inhibition	MAST4 % inhibition	MAST3 IC ₅₀ (μ M)
19	n.d.	90.8	76.1	1.01
25	n.d.	87.5	79.8	1.4
27	75.6	97.2	>88	0.29
28	36.9	80.6	75.6	2.4
35	>86	97.7	>88	0.24
AX13587	76	93.1	78.7	0.74

% Inhibition values are shown in the form of a heat map and compound structures can be found in Table 4. Also shown also are MAST3 IC₅₀ values calculated from the corresponding MAST3 % inhibition value. n.d. = not determined.

9. (a) Patricelli, M. P.; Szardenings, A. K.; Liyanage, M.; Nomanbhoy, T. K.; Wu, M.; Weissig, H.; Aban, A.; Chun, D.; Tanner, S.; Kozarich, J. W. *Biochemistry* **2007**, *46*, 350; (b) Patricelli, M. P.; Nomanbhoy, T. K.; Wu, J.; Brown, H.; Zhou, D.; Zhang, J.; Jagannathan, S.; Aban, A.; Okerberg, E.; Herring, C.; Nordin, B.; Weissig, H.; Yang, Q.; Lee, J.-D.; Gray, N. S.; Kozarich, J. W. *Chem. Biol.* **2011**, *18*, 699.
10. Deleuze-Masquefa, C.; Moarbess, G.; Khier, S.; David, N.; Gayraud-Paniagua, S.; Bressolle, F.; Pinguet, F.; Bonnet, P.-A. *Eur. J. Med. Chem.* **2009**, *44*, 3406.
11. Guillon, J.; Moreau, S.; Mouray, E.; Sinou, V.; Forfar, I.; Fabre, S. B.; Desplat, V.; Millet, P.; Parzy, D.; Jarry, C.; Grellier, P. *Bioorg. Med. Chem.* **2008**, *16*, 9133.
12. Heine, H. W.; Brooker, A. C. *J. Org. Chem.* **1962**, *27*, 2943.
13. Other kinases that gave <35% inhibition but are not shown in Table 5: AGK, ANP β , ATR, CASK, CDK11, CDK8, CDK5, CHK2, CLK2, CSK, DNAPK, eEF2K, EGFR, EphA1, EphA2, EphA7, EphB2, EphB4, Erk1, Erk2, FAK, FER, FYN, SRC, YES, ILK, IRAK1, IRAK4, KHS1, KHS2, LOK, MAP2K1, MAP2K2, MAP2K3, MAP2K4, MAP2K6, MAP3K2, MAP3K3, MAP3K4, MARK2, MARK3, MARK4, MET, MLK3, MRCK β , MST1, MST2, MST4, YSK1, NDR2, NEK6, NEK7, NEK8, NEK9, p38 α , p38 β , p70S6K, p70S6K β , PDK1, PHK γ 2, PKC α , PKC β , PKR, PRP4, ROCK1, ROCK2, RON, RSK2 domain2, SLK, SNRK, SRC, SRPK1, SRPK2, TAO1, TAO3, TLK1, TLK2, Wnk1, Wnk2, Wnk4, ZAK.
14. (a) Garland, P.; Quraishie, S.; French, P.; O'Connor, V. *Brain Res.* **2008**, *1195*, 12; (b) Sun, L.; Gu, S.; Li, X.; Sun, Y.; Zheng, D.; Yu, K.; Ji, C.; Tang, R.; Xie, Y.; Mao, Y. *Mol. Biol. (Mosk)* **2006**, *40*, 808.
15. Miduturu, C. V.; Deng, X.; Kwiatkowski, N.; Yang, W.; Brault, L.; Filippakopoulos, P.; Chung, E.; Yang, Q.; Schwaller, J.; Knapp, S.; King, R. W.; Lee, J. D.; Herrgard, S.; Zarrinkar, P.; Gray, N. S. *Chem. Biol.* **2011**, *18*, 868.
16. Structure of the desthiobiotin-ATP probe **AX9509**

